## Malaysian Journal of Analytical Sciences (MJAS)



Published by Malaysian Analytical Sciences Society

# THERMAL STABILITY AND POROSITY OF REDUCED GRAPHENE OXIDE/ZINC OXIDE NANOPARTICLES AND THEIR CAPACITY AS A POTENTIAL OXYGEN REDUCTION ELECTROCATALYST

(Kestabilan Haba dan Keliangan Partikel Nano Grafin Oksida Terturun/Zink Oksida dan Keupayaannya sebagai Pemangkin Elektro Tindakbalas Penurunan Oksigen)

Karthi Suresh and Farhanini Yusoff\*

Faculty of Science and Marine Environment, Universiti Malaysia Terengganu, 21030 Kuala Nerus, Terengganu, Malaysia

\*Corresponding author: farhanini@umt.edu.my

Received: 30 March 2020; Accepted: 2 May 2020; Published: June 2020

#### Abstract

Zinc oxide/reduced graphene oxide (ZnO/rGO) nanoparticle were synthesized through a facile one-pot method. The use of rGO was initiated due to presence of more active sites compared to graphene oxide (GO). Physical characterization such as Fourier transform infrared spectroscopy (FTIR) confirmed the presence of ZnO stretching peak in the spectrum of rGO, suggesting that nanoparticles coexisted as a component. Thermo-gravimetric analysis (TGA) confirmed the stability of nanoparticles as 68.91% of the nanoparticles remained after exposure to high temperature of 900 °C. The nanoparticles were under mesopore region when studied using Brunauer-Emmett-Teller (BET), with the pore volume of 10.4 nm. Drops of ZnO/rGO were drop-casted onto a bare glassy carbon electrode (GCE) to study the electrochemical behavior of the nanoparticles using cyclic voltammetry (CV) and electrochemical impedance spectroscopy (EIS) as well as oxygen reduction reaction (ORR). Electrochemical studies on the modified electrode of ZnO/rGO/GCE exhibited greater current responses, stable electron transfer and also lower charge transfer resistance compared to a bare GCE. The nanoparticles demonstrated the potential application as an electrocatalyst with high yield rate in (ORR). Hence, the nanoparticles could be used as a substitute for precious metal usage, such as platinum, in current production and overcoming high costs.

Keywords: electrochemistry, nanoparticle, electrolyte, graphene, zinc oxide

#### Abstrak

Nanopartikel zink oksida/grafin oksida terturun (ZnO/rGO) disintesis dengan cara satu pot. rGO digunakan kerana mempunyai tapak aktif yang banyak berbanding grafin oksida (GO). Pencirian fizikal yang dilaksanakan menggunakan spektroskopi inframerah transformasi Fourier (FTIR) mengesahkan kehadiran ZnO di spektrum rGO, yang mencadangkan kedua partikel ini wujud sebagai satu komponen sebati. Analisa gravimetrik terma (TGA) mencatatkan kestabilan nanokomposit dengan lebihan 68.91% di penghujung analisa 900 °C, dan nanokomposit disahkan sebagai komposit liang meso melalui keputusan analisa BET, dengan saiz liang 10.4 nm. Elektrod karbon berkaca (GCE) digunakan dan diubahsuai menggunakan ZnO/rGO dengan teknik salutan titisan kemudiannya dikaji pencirian elektrokimia menggunakan kitaran voltametri (CV), spektroskopi elektrokimia impedans (EIS) dan tindak balas penurunan oksigen (ORR) yang menunjukkan respon elektrik yang bagus dan pemindahan

### Suresh & Farhanini: THERMAL STABILITY AND POROSITY OF REDUCED GRAPHENE OXIDE/ZINC OXIDE NANOPARTICLES AND THEIR CAPACITY AS A POTENTIAL OXYGEN

REDUCTION ELECTROCATALYST

elektron yang stabil serta kurang rintangan pemindahan kuasa apabila dibandingkan dengan GCE. Komposit nano menunjukkan keupayaan pengganti sebagai pemangkin elektro dan kadar hasil tinggi di ORR yang berkemungkinan menjadi pengganti logam berharga seperti platinum dan dapat mengurangkan kos penghasilan.

Kata kunci: elektrokimia, nanopartikel, elektrolit, grafin, zink oksida

#### Introduction

Text The demand of energy for essential consumption increases tremendously in response to uncontrolled growth of the human population in the world. By focusing on renewable energy, fuel cells have been invented with platinum as the common material [1]. Despite its optimal energy yield, platinum is far more expensive compared to other precious metals. In addition, the electrode used in the production of fuel cells cannot be recovered completely and the amount of platinum used is extensive to reach the desired power densities, and this contributes to major economic issues [2]. Moreover, pollution occurs when using a platinum electrode, which releases carbon dioxide (CO<sub>2</sub>) during the reaction.

Therefore, the idea of producing a relatively inexpensive electrocatalyst that can be used as a substitute or an even better conductor than platinum, and with better stability and porosity has been put forward [3]. The synthesized nanoparticles consist of zinc oxide (ZnO) and reduced graphene oxide (rGO). Graphene is a two-dimensional carbon allotrope that has been considered as a research interest due to its unique structure and physicochemical properties. In this research, rGO was prioritized by reducing the synthesized graphene oxide (GO) using hydrazine hydrate through a one-pot method. The reduction of GO causes loss in the hydroxide (-OH) functional group, hence creating more active sites in the structure [4].

The unification of nanoparticles with graphene-related materials, in this case ZnO and rGO as nanoparticles have recently become a trend in research due to their enhanced functionalities that cannot be achieved by either component alone. Previous research on fabricating metal oxide/graphene nanoparticle enhanced the electrocatalytic activity [5].

The porosity and thermal stability of nanoparticles have been studied thoroughly as these criteria affect the electrochemical capacitance of nanoparticles. A pore volume that fits perfectly into the mesopore region of 2-50 nm is said to be optimal as energy density will be higher and applicable in electrochemistry. Thermal stability examines the strength if the nanoparticles can be used at higher temperature during energy production. These three as pects play a major role in the nanoparticles, especially when dealing with energy and electrochemistry as these properties affect the kinetics of ionic diffusion within the matrix, electron transfer, and capacitance of the nanoparticles [6]. Mesoporosity is preferred for better energy capacitance and electron transfer as a larger (macroporosity) or smaller (microporosity) size of particle directly affect energy density.

#### **Materials and Methods**

#### Chemicals and reagents

Graphite powder was used to synthesize GO using modified Hummers' method [7]. Zinc nitrate  $(Zn[NO_3]_2)$  and hydrazine hydrate were purchased from Sigma Aldrich to synthesize of nanoparticles using a one-pot method. All the chemicals purchased were of analytical grade reagents and no further purification was required. Deionized water of 18.2 M $\Omega$ cm was used for the purpose of diluting and washing the substances.

#### Physical characterization

The powder form of ZnO/rGO was characterized using several instruments to determine the purity of the obtained powder. The characterization was done using Fourier transform infrared spectroscopy (FTIR) to identify the functional groups available in the nanoparticles, scanning electron microscope (SEM) to study the morphological structure, thermal gravimetric analysis (TGA) to study the rate of mass loss in samples and thermal stability, and also Brunauer-

Emmett-Teller (BET) analysis to study the surface area and porosity of the synthesized nanoparticles.

#### Electrochemical characterization

To determine the electrocatalytic activity of the synthesized nanoparticles, cyclic voltammetry (CV), electrochemical impedance spectroscopy (EIS) and oxygen reduction reaction (ORR) were studied using a potentiostat galvanostat (PG) instrument. A glassy carbon electrode (GCE) was used as the modified electrode in this method. The electrode was polished using alumina oxide to ensure its purity. About 1 mg of ZnO/rGO powder was sonicated with 10 ml of deionized water for 30 minutes. Then, 10 µL of the solution was dropped onto the GCE and allowed to dry. After that, the electrocatalytic activity was studied with 5.0 mM of potas sium ferricyanide (K<sub>3</sub>[Fe(CN)<sub>6</sub>]) in 0.1 M of potassium chloride (KCl) electrolyte solution using the modified electrode with potential window of -0.2 to 0.8 V. For ORR, the electrolyte was purged with oxygen (O2) for 10 minutes for oxygen saturation condition.

#### Synthesis of graphene oxide

Graphene oxide (GO) was synthesized using modified Hummers' method [7, 8]. Graphite powder was added to 0.5 g of sodium nitrate (NaNO<sub>3</sub>) and concentrated sulfuric acid (H<sub>2</sub>SO<sub>4</sub>) in a volumetric flask that was kept under ice bath under continuous stirring for 30 minutes. Potassium permanganate (KMnO<sub>4</sub>) was gradually added into the solution and stirred for 2 hours. Next, the paste was slowly diluted with 45 mL of deionized water and the reaction temperature increased to 98 °C. The stirring was continued and further dilution with deionized water was done. Hydrogen peroxide (H<sub>2</sub>O<sub>2</sub>) was used to stop the reaction. About 5% of hydrochloric acid (HCl) and deionized water were used to rinse the solution and then centrifuged for purification. After centrifugation, the solution was filtered and dried under vacuum at room temperature [4].

#### Facile one-pot synthesis of ZnO/rGO

Zinc nitrate was added into a beaker containing 50 mL of deionized water and stirred in an ice bath for 1 hour. Later, 0.1 g of GO was mixed with 100 mL of

deionized water and stirred for 30 minutes. After that, 0.5 g of sodium hydroxide (in pallets) and 0.3 mL of hydrazine hydrate were added into the beaker and stirred vigorously for another 30 minutes. Hydrazine hydrate was added into the solution for further reduction of GO's hydroxyl functional group. The mixture was left overnight for precipitation. Then, the precipitate was filtered using a vacuum pump and washed with deionized water to adjust the pH to neutral. Finally, the precipitate was dried in an oven for 12 hours at 60 °C for further use.

#### **Results and Discussion**

The functional groups of all synthesized materials were studied using FTIR. The spectra of graphite, GO and ZnO/rGO are shown in Figure 1. Graphite (1a) possessed a tiny, almost unidentified peak at 1610 cm<sup>-1</sup> of C=C in its spectrum, describing its carbon characteristics. Other peaks were not identified in the spectrum(1a), possibly due to the miniscule width of the peak [9]. A broad peak of 3400 cm<sup>-1</sup> was observed in the spectra of GO in Figure 1(b) indicating the presence of hydroxyl (-OH) functional group, which later shrank in the spectrum of ZnO/rGO (1c). This proved that reduction occurred as well as the elimination of functional groups. The peaks at 1718 cm<sup>-1</sup> and 1623 cm<sup>-1</sup>, and also 1225 cm<sup>-1</sup> and 1054 cm<sup>-1</sup> in the spectrum of GO represent the functional groups of C=O (amide), aromatic C=C, and stretching vibration of C-OH groups, respectively [8]. Meanwhile in the ZnO/rGO spectrum, there were only peak at 1589 cm<sup>-1</sup> for C=O (amide) and 1384 cm<sup>-1</sup> for aromatic C=C originated from GO. Other functional groups mainly C-OH groups were reduced during reduction process. The peak at 476 cm<sup>-1</sup> in Figure 1(c) shows the presence of ZnO in the spectra of ZnO/rGO, indicating the co-existence of nanoparticles. The spectra of FTIR was further supported by the data of X-ray diffraction (XRD) presented in previous articles [5].

Scanning electron microscope (SEM) explains the morphological structure of the nanoparticles produced. Figure 2(a) shows the image of graphite, which can be seen as flaky layers, and later changed its structure into a rough and wrinkled surface (Figure 2b) when synthesized into GO. The microscopic image of

ZnO/rGO shown in 2(c) consist of a sharp tentacle-star-like structure observed coating the GO sheet which now exists as rGO [5]. From these morphological images, it can be concluded that the desired product is achieved with a larger surface area and more active sites are produced, which are useful for increased catalytic activity [10].

In TGA, the nanoparticles were exposed at 30 °C and heated constantly at the range of 10 °C/min in N2 atmosphere until the maximum stop temperature of 900 °C. As observed in Figure 3(a), first degradation occurred consistently up to about 100 °C for all graphite, GO, and ZnO/rGO with the percentage loss of mass of 4.55%, 17.88%, and 8.21%, respectively. This indicates the loss of water vapors, hydroxyl (-OH) groups and residuals in the nanoparticles [11]. Graphite showed a steady decrease until 620 °C, and a rapid degradation was later observed until complete combustion at 850 °C. This might be due to the combustion of carbon-carbon skeletons [12]. A significant drop of GO mass, (approximately 49.60%) was observed at 670 °C which might be resulted from further loss of hydroxyl groups attached to the graphene layer [13]. Meanwhile, ZnO/rGO was stable throughout the end temperature with a loss of mass about 31.09%. Therefore, it is proved that the stability of ZnO/rGO nanoparticles is better compared to GO and the reduction of GO gives better thermal stability [5, 14, 15].

The BET analysis measures the specific surface area of nanoparticles by studying the physical adsorption of  $N_2$  of the material. In this analysis, the bath temperature used was 78 K. The result of the analysis (as tabulated in Table 1) show that the surface area for GO is the greatest amongst other materials, with a surface area of  $304.43~\text{m}^2/\text{g}$ , whereas ZnO/rGO has a surface area of  $35.62~\text{m}^2/\text{g}$ . Lower surface area could be linked with the drastic reduction of hydroxyl functional group when one-pot synthesis was carried out. However, GO is categorized as macropores with pore volume of  $1.425~\text{cm}^3/\text{g}$ , which is about 143 nm when the Barrett-Joyner-Halenda (BJH) pore volume was studied. ZnO/rGO recorded the pore volume of  $0.104~\text{cm}^3/\text{g}$ , which is in the mesopore region of the analysis.

Macropores are not suitable in the study of electrochemistry as it may disrupt electron transfer due to larger pore size. Mesoporosity is the optimal condition in the aspect of energy and capacitance, as well as electron transfer [16]. The condition is applicable in quick energy transfer and storage. Based on the physisorption isotherm plotted in Figure 3(b), the hysteresis loop of H2 is for GO and the hysteresis loop for H1 is for ZnO/rGO.

CV explains the electrochemical efficiency of the nanoparticles in Figure 4(a). A bare GCE was used which was later modified into a nanoparticle-deposited modified electrode by drop-casting GO and ZnO/rGO. The current used in this study was 50 mV standard for all three experiments. The analysis showed that ZnO/rGO possessed greater current responses compared to the bare GCE and GO. The peak potential separation (  $\Delta E_P = E_{Anodic\ peak} - E_{Cathodic\ peak}$ ) of ZnO/rGO is identical to GO and bare GCE at the value of  $\Delta E_P$  = 150 mV, suggesting that the electron transfer is stable and rapid with a reversible process [5, 17].

EIS is conducted to determine the electron mass transfer between the electrolyte and electrode surface. Charge transfer resistance (R<sub>ct</sub>) represents the kinetic resistance of charge transfer in the redox reaction between the electrode and the electrolyte [18]. As seen in Figure 4(b), the R<sub>ct</sub> that is represented the semicircle in the Nyquist plot becomes smaller. ZnO/rGO modified electrode possessed discrete and incomplete semicircle compared to the bare GCE electrode, hence providing data that the R<sub>ct</sub> is higher in the bare GCE compared to the modified electrode Table 2 tabulates the data of R<sub>CT</sub> obtained from the software based on the Nyquist plots of experimented modified electrodes. The  $R_{\text{ct}}$  decreased as the bare GCE electrode was modified to GO and then to ZnO/rGO. Lower R<sub>CT</sub> indicates less resistance in electron transfer between the electrode surfaces [19, 20].

Figure 5 portrays the cyclic voltammogram of the modified electrode ZnO/rGO/GCE in ORR studied under condition of 0.1 M of potassium hydroxide (KOH) solution as the electrolyte. The study of ORR is important in electrochemical analysis as it provides

information on catalytic activity in reduction process [6, 21]. Two electrolytebases were prepared; one was purged with  $N_2$  and another base was purged with  $O_2$ , for 10 minutes. The voltammograms plotted in Figure 5(b) do not show any peak in nitrogen saturated electrolyte, indicating no redox reaction occurred in that condition. A single cathode reduction peak was observed in oxygen saturated electrolyte, indicating an irreversible process of  $O_2$  reduction at the

electrocatalyst [3]. The ZnO/rGO/GCE modified electrode (Figure 5a) shows better electrocatalytic performance compared to the GO/GCE modified electrode. The cathode peak observed indicates higher and better current density of the ZnO/rGO/GCE electrode compared to the GO/GCE electrode. This shows the high affinity of the electrode towards O<sub>2</sub> saturated condition [16].

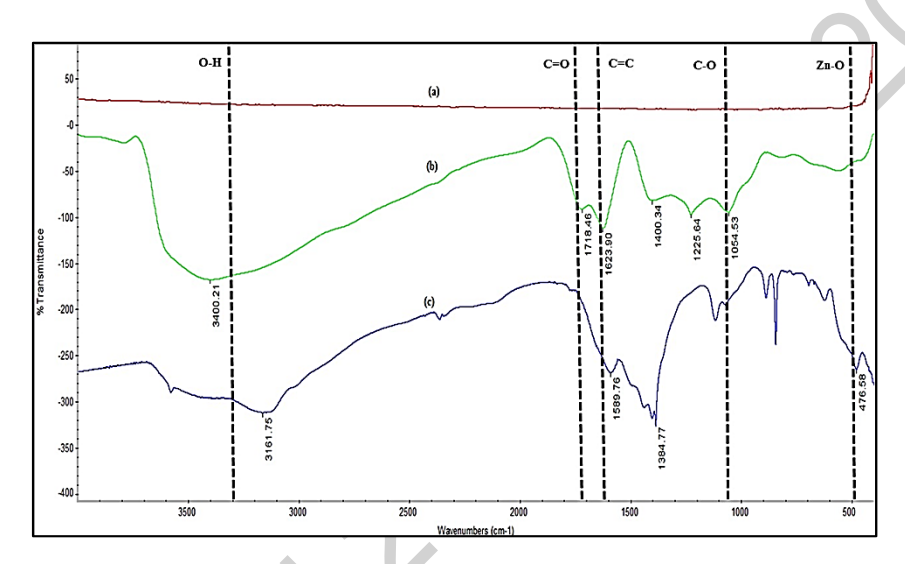


Figure 1. FTIR spectra of (a) graphite, (b) GO, and (c) ZnO/rGO

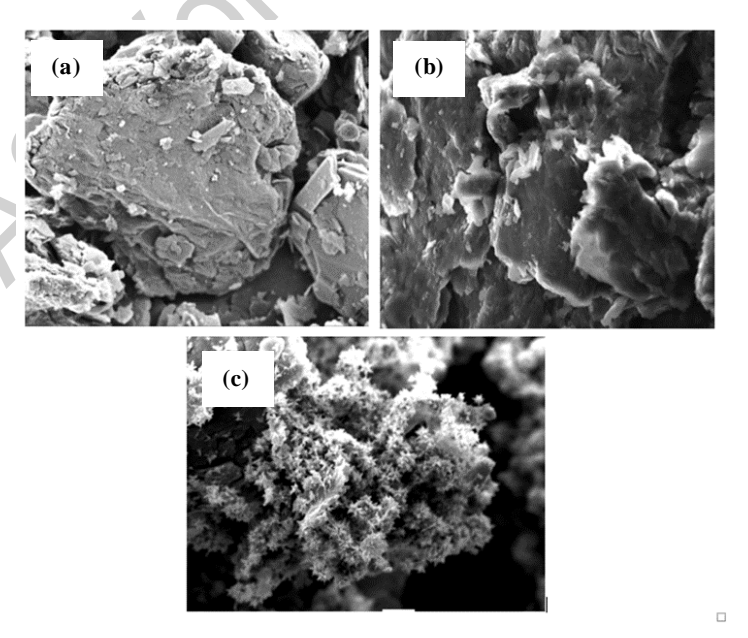


Figure 2. SEM images of (a) graphite, (b) GO, and (c) ZnO/rGO

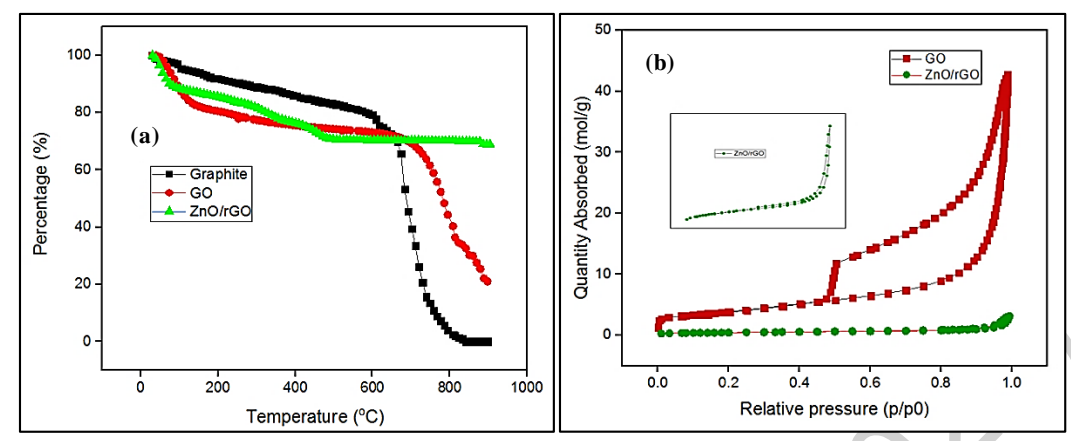


Figure 3. (a) TGA comparison between GO and ZnO/rGO and (b) BET isotherm graph, (Inset) a clearer graph of ZnO/rGO

Table 1. BET and BJH analyses for surface area, pore volume, and pore adsorption diameter

Sample	BET Surface Area (m²/g)	BJH Pore Volume (cm³/g)	Average Adsorption Pore Diameter (4V/A)
GO	304.43	1.425	194.91
ZnO/rGO	35.62	0.104	121.51

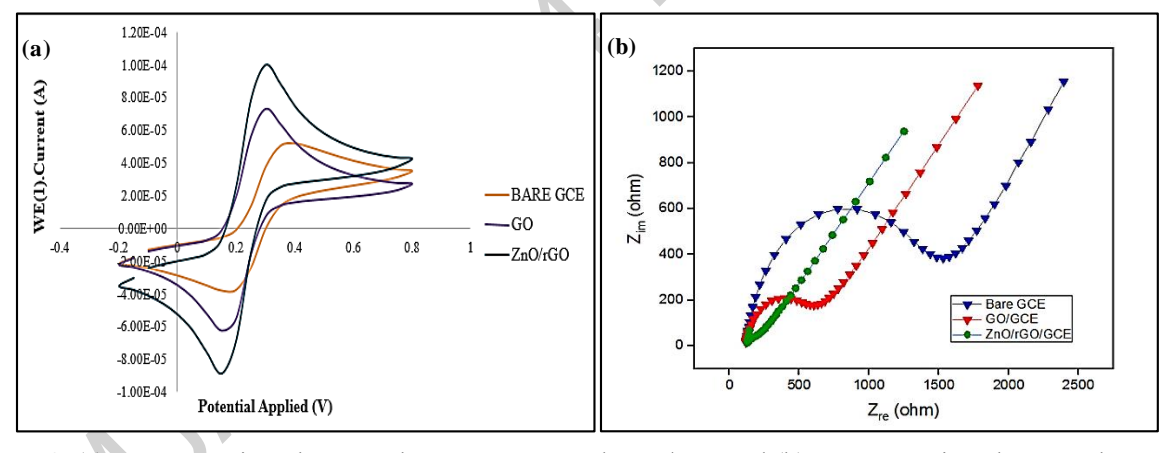


Figure 4. (a) CV comparison between bare GCE, GO, and ZnO/rGO and (b) EIS comparison between bare GCE, GO, and ZnO/rGO

Table 2.  $R_{ct}$  values of bare GCE, GO/GCE, and ZnO/rGO/GCE

Electrodes	Charge Transfer Resistance, $R_{CT} \left( \Omega cm^2 \right)$	
Bare GCE	1586.03	
GO/GCE	698.58	
ZnO/rGO/GCE	160.18	

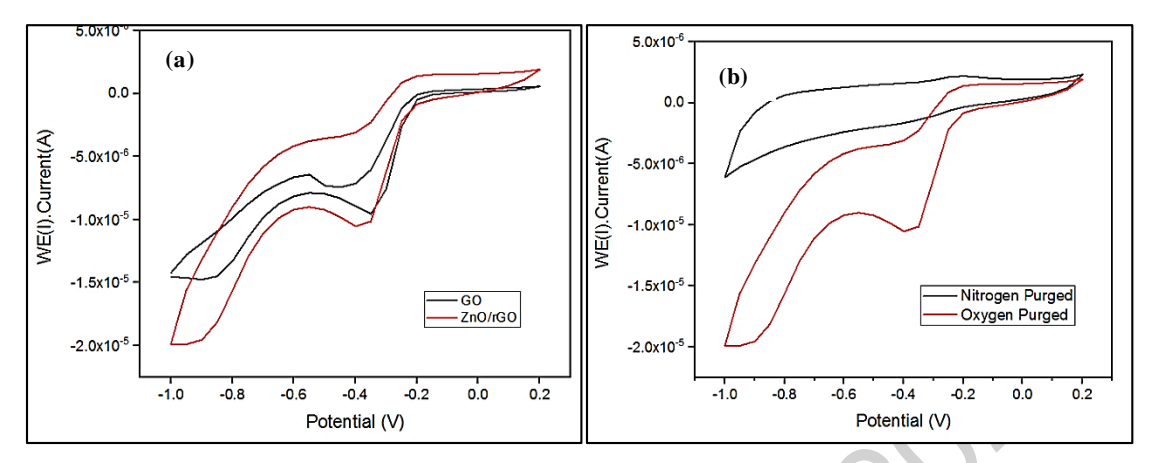


Figure 5. a) CV of ORR of GO with ZnO/rGO and (b) comparison of ZnO/rGO voltammetry with both  $N_2$  and  $O_2$  purged into the electrolytes

#### Conclusion

The synthesis of ZnO/rGO powder was carried out through a facile one-pot synthesis method. The analysis of FTIR, SEM, TGA, and BET showed that the desired product was successfully synthesized. The FTIR spectra of ZnO/rGO show a great reduction in the broad peak of 3400 cm<sup>-1</sup> compared to the spectra of GO, proving that reduction occurred by the elimination of hydroxyl (-OH) functional groups due to the addition of Zn(NO<sub>3</sub>)<sub>2</sub> and hydrazine hydrate. The TGA analysis showed that ZnO/rGO is thermally stable and suitable for use at high temperature condition. The acquired results of CV show greater current responses with rapid and stable electron transfer with the value of  $\Delta E_P$  obtained and smaller  $R_{CT}$  value for the modified electrode, indicating lower resistance during electron transfer. The ORR analysis portrayed an increase at the cathode peak of ZnO/rGO ascribing optimum surface area to volume ratio and possessing high affinity toward oxygen. The nanoparticles are believed to be a better option to be used as a potential electrocatalyst with better stability as proven in this study.

#### Acknowledgement

Authors wish to thank the Ministry of Education Malaysia for the Fundamental Research Grant Scheme (FRGS Vot: 59472) provided as financial support in conducting the research. Authors also acknowledge the Faculty of Marine Science and Environment, University Malaysia Terengganu for the research

facilities and instrumentation provided.

#### References

- 1. Abdalla, A. M., Hossain, S., Azad, A. T. and Petra, P. M. I. (2018). Nanomaterials for solid oxide fuel cells: A review. *Renewable and Sustainable Energy Reviews*, 82: 353-368.
- 2. Wang, Y., Leung, D. Y. C., Xuan, J. and Wang, H. (2017). A review on unitized regenerative fuel cell technologies, Part B: Unitized regenerative alkaline fuel cell, solid oxide fuel cell, and micro fluidic fuel cell. *Renewable and Sustainable Energy Reviews*, 75: 775-795.
- 3. Muhamad, N. B., Khairul, W. M. and Yusoff, F. (2019). Synthesis and characterization of poly(3,4-ethylenedioxythiophene) functionalized graphene with gold nanoparticles as a potential oxygen reduction electrocatalyst. *Journal of Solid State Chemistry*, 275: 30-37.
- 4. Stankovich, S., Dikin, D. A., Piner, R. D., Kohlhaas, K. A., Kleinhammes, A., Jia, Y. and Wu, Y. (2007). Synthesis of graphene-based nanosheets via chemical reduction of exfoliated graphite oxide, *Carbon*, 45: 1558-1565.
- 5. Yusoff, F., Khing, N. T., Hao, C. C., Sang, L. P., Basyirah, N. A. and Saleh, N. M. (2018). The electrochemical behavior of zinc oxide/reduced graphene oxidecomposite electrode in dopamine. *Malaysian Journal of Analytical Sciences*, 22(2): 227-237.

- Chen, Y. L., Hu, Z. A., Wang, H. W., Zhang, Z, Y., Yang, Y. Y. and Wu, H. Y. (2011). Zinc oxide/reduced graphene oxide composites and electrochemical capacitance enhanced by homogeneous incorporation of reduced graphene oxide sheets in zinc oxide matrix. *The Journal of Physical Chemistry*, 115(5): 2563-2571.
- 7. Hummers, W. S. and Offeman, R. E. (1958). Preparation of graphitic oxide. *Journal of the American Chemical Society*, 80(6): 1339.
- 8. Teymourian, H., Salimi, A. and Khezrian, S. (2013). Fe<sub>3</sub>O<sub>4</sub> magnetic nanoparticles/reduced graphene oxide nanosheets as a novel electrochemical and bioeletrochemical sensing platform. *Biosensors and Bioelectronic*, 49: 1-8.
- 9. Du, W., Lu, J., Sun, P., Zhu, Y. and Jiang, X. (2013). Organic salt-assisted liquid-phase exfoliation of graphite to produce high-quality graphene. *Chemical Physics Letters*, 568-569: 198-201.
- Deemer, E. M., Kumar, P., Manciu, F. S., Botez, C. E., Hodges, D. R., Landis, Z. and Chianelli, R. R. (2017). Consequence of oxidation method on graphene oxide produced with different size graphite precursors. *Materials Science & Engineering B*, 224: 150-157.
- 11. Papageorgiou, D. G., Kinloch, I. A. and Young, R. J. (2017). Mechanical properties of graphene and graphene-based nanoparticles. *Progress in Materials Science*, 90: 75-127.
- 12. Zaghib, K., Song, X. and Kinoshita, K. (2001). Thermal analysis of the oxidation of natural graphite: Isothermal kinetic studies. *Thermochimica Acta*, 371(1-2): 57-64.
- 13. Ryu, S. H. and Shanmugharaj, A. M. (2014). Influence of hexamethylene diamine functionalized graphene oxide on the melt crystallization and properties of polypropylene nanoparticles. *Materials Chemistry and Physics*, 146(3): 478-486.

- 14. Tiwari, A. and Hihara, L. H. (2009). Thermal stability and thermokinetics studies on silicone ceramer coatings: Part 1-inert atmosphere parameters. *Polymer Degradation and Stability*, 94(10): 1754-1771.
- 15. Huang, S. and Sheng, J. J. (2017). An innovative method to build a comprehensive kinetic model for air injection using TGA/DSC experiments. *Fuel*, 210: 98-106.
- 16. Yusoff, F., Mohamed, N., Aziz, A. and Ghani, S. A. (2014). Electrocatalytic reduction of oxygen at perovskite (BSCF)-MWCNT composite electrodes. *Materials Sciences and Applications*, 5(04): 199-211.
- 17. Nicholson, R. S. (1965). Theory and application of cyclic voltammetry for measurement of electrode reaction kinetics. *Analytical Chemistry*, 37(11):1351-1355.
- Palanisamy, S., Ezhil Vilian, A. T. and Chen, S. M. (2012). Direct electrochemistry of glucose oxidase at reduced graphene oxide/zinc oxide composite modified electrode for glucose sensor. International Journal of Electrochemical Science, 7(3): 2153-2163.
- 19. Tehrani, R. M. A., Ghadimi, H. and Ab Ghani, S. (2013). Electrochemical studies of two diphenols isomers at graphene nanosheet-poly(4-vinyl pyridine) composite modified electrode. *Sensors and Actuators, B: Chemical,* 177: 612-619.
- Yusoff, F., Aziz, A., Mohamed, N. and Ghani, S. A. (2013). Synthesis and characterizations of BSCF at different pH as future cathode materials for fuel cell. *International Journal of Electrochemical Science*, 8: 10672-10687.
- 21. Yu, J., Liu, Z., Zhai, L. and Huang, T. (2016). Reduced graphene oxide supported TiO<sub>2</sub> as high performance catalysts for oxygen reduction reaction. *International Journal of Hydrogen Energy*, 41(5): 3436–3445.